

Random packing of disks in two dimensions

Einar L. Hinrichsen, Jens Feder, and Torstein Jøssang

Department of Physics, University of Oslo, Box 1048, Blindern, 0316 Oslo 3, Norway

(Received 24 October 1989)

The geometry of a random dense packing of disks of equal size obtained by compacting a random sequential adsorption configuration is discussed. The configuration is shown to be without any long-ranged order, and no local configurations of ordered domains were found. The fraction of area covered by disks is $\theta=0.772\pm 0.002$, and the number of contacts per disk are 3.02 ± 0.03 . It is argued that this random packing is a stable configuration close to the random loose-packed limit in two dimensions. The packing fraction of the compacted packing is close to a prediction we make of $\theta=0.78$ for a random loose-packed configuration. Several statistical distributions calculated from the limiting geometry is studied. Both the area and circumference distributions of the Voronoi-Dirichlet polygons could be fitted to Γ distribution functions.

I. INTRODUCTION

Packing spheres of equal radii in a two-dimensional array has a long history, dating back to Kepler in 1619.¹ In the last 30 years packings in two and three dimensions have been studied extensively, in part because they serve as useful models for a variety of physical systems. The interest in three-dimensional packings is due to the fact that they can serve as models for the molecular nature of fluids, glasses, and amorphous materials.²⁻⁵ The macroscopic granular properties of powder and porous media^{6,7} have also been modeled by sphere packings.

The two-dimensional packings have often been studied as an introduction to a three-dimensional problem,⁸⁻¹² since two-dimensional geometry is more easily handled than the three-dimensional one. However, these packings have also been used as models for purely two-dimensional phenomena like the clustering of bacteria or the adsorption of monomolecular layers of large molecules on various surfaces.¹³⁻¹⁷ We are interested in random geometries because many of the physical processes that we are studying, like fluid flow in porous media,¹⁸ take place in a random geometry. In order to understand these processes, we feel the necessity to have a good understanding of the geometry specifying the boundary conditions for these processes. We are also interested in processes that create such random geometries, such as the adsorption of large molecules on a surface,¹⁶ and the distribution of proteins in cell membranes.¹⁹

The aim of the work presented here was to study a compaction process of nonoverlapping disks filling a surface, and to characterize the resulting geometry. Our starting point was a surface filled with disks generated by the random sequential adsorption algorithm.²⁰ Next, the disks started swelling (or equivalently the surface started to shrink) following a procedure we will describe in Sec. III. In order to obtain a stable configuration differing from any ordered structure, the compaction algorithm was designed to keep the configurations maximally random through the entire process. The dynamics of our model resembles the model of Hasegawa and Tanemura²¹

for the process of forming territories among animals.

In both two and three dimensions, three different limits of the packing fraction are of interest. The first limit is the configuration with the maximum packing fraction—the *close-packed* (CP) configuration—with a packing fraction $\theta_{CP}=\pi/\sqrt{12}=0.9069\dots$ in two dimensions and $\theta_{CP}=\pi/\sqrt{18}=0.7405\dots$ in three dimensions. The packing fraction (or coverage in two dimensions), is the fraction of space filled by spheres. Then there are two limits called the *random closed-packed* (RCP) and the *random-loose-packed* (RLP) configurations. The definitions of these concepts are nontrivial, and this will be discussed in Sec. II. In the same section we will also give an overview of the general problem of packing disks, as well as discuss other concepts developed in order to describe random geometries.

The procedure we used for comparing a packing of disks is described in Sec. III. In Sec. IV we analyze the dynamics of the compaction procedure. The result of implementing this procedure is a configuration that is stable in the limit of infinite “time.” The convergence to this limiting configuration was slow, but by extrapolating the coverage to an infinite number of iterations, we could estimate the coverage of this configuration to be $\theta=0.772\pm 0.002$. In Sec. V we argue that the limiting configuration is both maximally random and stable. The coordination number found for this configuration was $z=3.02\pm 0.03$. A value $z=3$ is the lowest possible for the coordination number since all disks must have three disks in contact for the configuration to be stable. In the compacted configuration we generated, the disks are stable except for cases where one or a few disks are free to move in an environment confined by a rigidly locked structure. Our procedure generates such configurations rather frequently, a fact that is somewhat surprising. The most recent literature more or less agrees upon $\theta=0.82\pm 0.02$ as the coverage for a RCP configuration.²² Since our configuration is at the lower limit of stability, we think that our configuration is very close to the RLP limit. The packing fraction of the limiting configuration is close to our prediction of $\theta=0.78$ for a RLP

configuration, based on a theory of Bideau *et al.*²²

In Secs. VI and VII we discuss geometrical features of the limiting configuration associated with our compactification procedure. In Sec. VI we discuss the hole-size distribution for the compact configuration generated, and in Sec. VII we analyze the statistical distributions of the Voronoi-Dirichlet (VD) division of space for these cases.

II. RANDOM DISK PACKINGS

In three dimensions the RCP configuration can be experimentally obtained by shaking containers filled up with ball bearings. The resulting coverage is then extrapolated to eliminate finite-size effects, resulting in a packing fraction $\theta_{\text{RCP}}=0.6366\pm 0.0004$ for steel ball bearings,^{4,23} as well as for ball bearings of other materials. The RLP configuration is less reproducible but has been obtained experimentally by pouring steel ball bearings into a container with rough walls without shaking,²³ giving a packing fraction $\theta_{\text{RLP}}=0.60\pm 0.02$. Even though these experimental results are well agreed upon for ball bearings, it is not clear that they represent the limiting value for idealized sphere packings¹⁰ (packings where, e.g., friction between the spheres is neglected). Simulation of these packings on a computer generally gives a greater variety of packing fractions, ranging from $\theta=0.61$ generated by a sequential addition algorithm,⁵ up to $\theta=0.665$ generated by a cooperative arrangement algorithm.²⁴ Attempts have been made to calculate θ_{RLP} and θ_{RCP} by various statistical geometrical approaches. Gotoh and Finney²⁵ found $\theta_{\text{RLP}}=0.61$ and θ_{RCP} in the interval $[0.6357, 0.6472]$, while Berryman¹⁰ found $\theta_{\text{RCP}}=0.64\pm 0.02$.

In two dimensions the situation is even less clear. This is first of all due to the lack of precise definitions of the characteristics of RLP and RCP configurations.^{10,26} The main difficulty with obtaining a random dense packing in two dimensions is linked with the lack of *frustration* between short- and long-range order. In three dimensions the locally most dense configuration—the tetrahedron—will not fill the space. The locally dense configuration is not the preferred one if one wants a global maximum of the packing fraction. This frustration between short- and long-range order is the principal reason for the observed structure of random dense packings in three dimensions, since most packing processes try to maximize the density locally.

In two dimensions such as frustration between short- and long-range orders does not exist. Locally the triangular agreement is the densest configuration, and it also tiles the space. The most used packing algorithms are grown algorithms, the most common being a growth algorithm due to Bennet,⁵ where a new particle is added as close as possible to an initial seed. In order to introduce frustration in two-dimensional packings and to mimic some of the behavior found in three dimensions, different approaches have been used. The initial seed of growth may be a central disk larger than the other disks, or the growth may start from an irregular boundary.^{27,28} Packings have also been simulated in curved space.^{29–31} Several studies have been made of the phase diagram,

coordination number, and packing fraction in packings of hard disks with two different sizes as the concentration and diameter ratio are varied.^{9,11,22,32–34} Packings in two dimensions have also been made with regular polygons³⁵ instead of disks. Even though packings in two dimensions with frustration introduced in one of these ways make a closer contact with three-dimensional packings than packings of disks of equal size, the existence of two-dimensional RLP and RCP configurations in packings of equally sized disks is still an open question. Some authors think that the RCP configuration may identify the transition from liquid to solid of fatty acids adsorbed on a contracting film.^{15,17}

In order to discuss these packings, we should have a clear definition of the different packing limits. Such a definition should be purely geometrical, and not linked to any particular thermodynamic quantity of a hard-sphere fluid like the singularity in the equation of state,^{6,36} as argued by Berryman,¹⁰ although such relations are of interest.

In order to define what we mean with RLP and RCP configurations, we must first consider what we mean by a *random* or *maximal random* configuration, a concept first introduced in a thesis by R. Ben Aim in 1970 (see reference in Ref. 11). We will also define what we mean by a *stable* and a *dense* configuration.

We define *maximal random configuration* as a configuration without any short- and long-range order. The long-range order may be defined in terms of radial and angular two-particle correlation functions showing no correlations. The lack of short-range order is more subtle. Many packing algorithms generate small zones with a regular triangular structure, where a disk will have six neighboring disks at contact. But ordering may also refer to the square lattice.²² Packings constructed by sequential addition of disks under the influence of a uniaxial field create large domains with a distorted square lattice structure.^{27,28} For a configuration to be maximal random, no such short-range ordering should exist—or to be more precise—the contribution to the coverage from such arrangements should vanish in the thermodynamic limit where the size of the system goes to infinity. This definition is similar to the definition given by Berryman¹⁰ stating that a random configuration contains neither short- nor long-range correlations. We have been more precise with the definition of no short-range correlation, since that is the crucial point in going from a random to a crystalline structure. This point has been neglected in many of the earlier works.

We also introduce the concept of *stable configurations*. A stable configuration is a *local maximum* of the coverage in the space of all configurations. Such a configuration is stable in the sense that if we want to make it denser, it must first be expanded. The expansion needed may only give an infinitesimal increase in the coverage. Therefore this stability requirement does not imply stability against thermal vibrations (of molecular structure) or a general shaking procedure (for granular materials). In fact, in a flat two-dimensional space it is believed that only the triangular lattice configuration [see Fig. 1(d)] is stable in the alter case. The reason being the

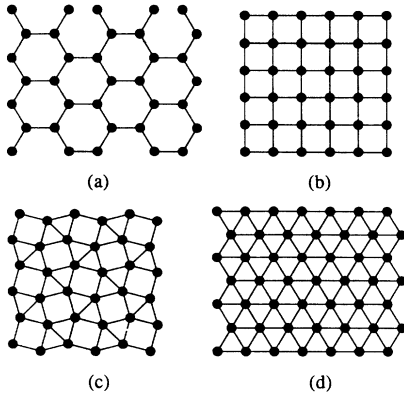


FIG. 1. Regular two-dimensional packings with the highest coverage for coordination number $z = 3, 4, 5$, and 6 (taken from Ref. 38).

lack of frustration between short- and long-range correlations.

A stable configuration as we have defined it is therefore not likely to be the limiting configuration of the contraction procedure described by Stillinger *et al.*⁸ This was noticed in experiments with silicon O rings on a contracting rubber film by Quickenden and Tan,¹⁵ and in computer simulations by Mason.³⁷

There exists only 11 regular two-dimensional packings that are stable in the sense defined above.³⁸ These packings have a coverage θ ranging from $\theta = 0.390\,675$ and up to $\theta_{\text{CP}} = 0.906\,900$ for the closed-packed (CP) configuration in Fig. 1(d). The coordination number ranges from $z = 3$ up to the only regular configuration with $z = 6$. In Fig. 1 we show packings with the highest coverage for each coordination number.

Last we define a *dense packing* as a packing where no movable disk may be moved to create holes sufficiently large for additional disks. Of the four regular packings in Fig. 1, only Fig. 1(a) is not dense, since there it is room enough to insert more disks.

Using these definitions we may now define RCP and RLP configurations as the configurations with the maximal or minimal coverage, respectively, of all maximal random, dense, and stable configurations. Note that this definition is purely geometrical without reference to external fields, frictional forces at points of contact, or thermodynamic quantities. Our definition of RLP configurations is not analogous to three-dimensional configurations generated by experiments because they are stable in a uniaxial field. Friction among the spheres also plays an important part in experiments.

There have been many attempts to construct random close packings in two dimensions, mostly by simulations; however, a few experiments have also been carried out. These algorithms may be divided into three classes: growth models in a central or uniaxial field starting with a seed,^{14,27,28,32,39} compaction of a random open configuration,^{8,11,15,29,37} and lastly, diluting a CP configuration and relaxing the disks into the created voids.⁴⁰ The results of these simulations and experiments seem to fall in the range $0.80 < \theta < 0.89$, as compiled by Berryman.¹⁰ Also the conclusions drawn by various au-

thors from their works are different. Some claim that $\theta = 0.82 \pm 0.02$ is an upper limit to the coverage for a RCP configuration; others claim that the same value is a lower limit. The distinction between or definitions of RLP and RCP configurations are also unclear in the literature. Finally, most of the work done lacks a thorough investigation of the geometry of these configurations, especially an identification of crystalline zones. There are some exceptions like Kausch *et al.*¹⁴ who, from a simulation of a growth process under the influence of a central field, found small triangular crystalline domains. They tried to correct the observed packing fraction for these domains, leading to $\theta_{\text{RCP}} = 0.82$. Visscher and Bolsterli²⁷ simulated growth under the influence of gravitational force, and found after an initial random growth, large domains of nearly square structure tilted at about 45° from the vertical. The increase of the coverage from $\theta = \pi/4 = 0.785$ for a square packing as the one in Fig. 1(b), to the observed value of $\theta = 0.82$ was ascribed mainly to the higher density in the grain-boundary region. Visscher and Bolsterli also claimed that Kausch *et al.*¹⁴ should see these domains for large clusters when a central force acts more as a uniaxial force.

There have been several theoretical approaches based on various statistical geometrical assumptions, all leading to values close to $\theta_{\text{RCP}} = 0.82$.^{6,10,22,41-43} Some of these approaches⁴¹⁻⁴³ assume a coordination number $z = 4$. This value is most probably correct when disks are added one by one as densely as possible under the influence of a central or uniaxial field. In this case each new disk added needs two contacts to be stabilized. But in a collective reconstruction process, this value may be lower. The lowest value any stable packing can have is $z = 3$, since each disk must be supported by a minimum of three neighboring disks in order to be blocked from any movement. Also, the angle that any pair of these neighbors make with the center disk must be less than π for the center disk to be blocked or stable. If this is not the case, the central disk could move without moving any of its neighbors.

One of the main tools in characterizing the geometry of a random disk packing is the statistical distributions of network quantities that may be derived from the different networks possible to construct from the positions of the disk centers. The first network is based on the Voronoi-Dirichlet (VD) division of space. This division is defined as follows: Around every disk center we find the set of points closer to this center than to any other disk center. This set of points defines the interior of a convex polygon. The VD network is defined from the edges of these polygons. By definition each VD cell contains one and only one disk. This tessellation is shown in Fig. 2 for the random sequential adsorption configuration. In a close-packed configuration the VD tessellation consists of regular hexagons. Another tessellation of space is the dual of the VD network.^{28,32} The vertices of this network are at the centers of the disks. Nearest-neighbor pairs (also called contiguous pairs^{3,20}) defined from the VD tessellation as a pair of disks defining an edge in a VD polygon, are connected with a line segment. This dual network of

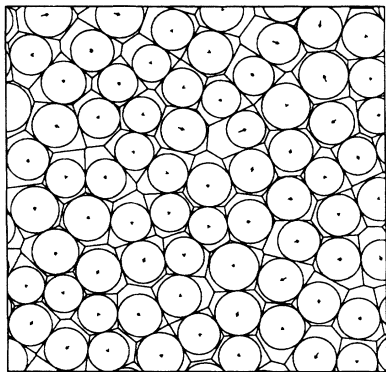


FIG. 2. The figure shows the first iteration step for the region within the inner frame in Fig. 4. The network is the VD network for the starting configuration. The circles are the largest circles possible to inscribe in each polygon. The segments with an arrow represent the disk movements. The starting points are at the disk centers defining the VD polygons and the end points are at the centers of the circles shown.

the VD network is a tessellation of space made out of triangles only, since each vertex in the VD network is defined by three disks.²⁰

Another network representation often studied in connection with random dense packings relies on the real contacts between disks.^{22,28} In the triangular network defined above, only lines going through real contacts are retained. All the remaining links will therefore have the same length equal to the disk diameter d . This new network consists mainly of polygons, but unlike the two other networks, it may exhibit some isolated sites and dead ends. If each disk is stable in the sense discussed above, this network will be completely connected without dead ends. In discussing the stability of dense packings, this network is probably the most natural. But for reasons that will become clear later, we cannot discuss the statistics of this network in our limiting configuration. Theoretical estimates for the coverage of an RCP configuration, are often based on statistical and topological constraints of these different tessellations.^{6,22,42}

III. DESCRIPTION OF THE PROCESS

As a starting configuration for the contraction of the surface, we used the *random sequential adsorption* (RSA) configurations described in Ref. 20. This configuration is generated by sequentially adding disks randomly onto a surface. A disk is irreversibly adsorbed on the substrate if it does not overlap any disks already there. If, however, the new disk overlaps any disk already adsorbed, the disk is removed and a new trial is made. This process continues until the surface is jammed, i.e., until there is no room for another disk. At this stage the fraction of the area occupied by disks, or the coverage, is $\theta = 0.5472 \pm 0.0002$. The geometry of this jammed configuration is well characterized.²⁰ The RSA configuration is a random packing of equal nonoverlapping disks without any long-range order. The two-

particle correlation function has a logarithmic divergence at contact, and there is no other short-ranged structure; in particular, there are no hexagonal nuclei in the RSA configuration. Even if the RSA configuration is jammed, it is not stable because many disks may easily be moved to create holes sufficiently large to accommodate new disks. The RSA model describes some of the essential features in protein adsorption on a surface.¹⁶

Starting with the RSA configuration, the surface is “contracted” homogeneously without any preferred directions in contrast to algorithms that use axial or central force fields. This contraction procedure is done iteratively in a way that ensures that the configuration is manifestly random and homogeneous during the whole process.

One iteration step is as follows: First a VD polygon is constructed around every disk. Each disk center is then moved to the center of the largest inscribed circle in the respective polygons, as indicated by the arrows in Fig. 2. Then all the disk radii are increased with the same amount until the first disk pair is in contact. A new configuration with somewhat higher coverage is obtained, and the whole process is repeated. The iteration procedure is somewhat similar to the one used by Hasegawa and Tanemura²¹ in their model of spatial patterns of animal territories, but they used the average coordinates of the vertices defining a VD polygon as the new disk center.

This iteration process is equivalent to a uniform contraction of the surface where the particles have a weak repulsive force in addition to the hard-core repulsion. We will argue that the limiting configuration after having repeated this iteration procedure infinitely many times, is a random dense packing close to the RLP limit.

In practice, we have carried out our simulations on a unit square with periodic boundary conditions in both x and y directions. The area of a particle is always measured relative to this unit square, and the disk diameter increases as the structure is compacted. We started out with 66 completely jammed RSA configuration made out of disks with a relative area of $a = 0.0002$. The average coverage of these configurations was $\theta = 0.5472 \pm 0.0002$. This estimate of the coverage for the two-dimensional RSA of disks is as far as we know that most precise value reported. The procedure of generating a completely jammed RSA configuration is explained in Ref. 20. Next we performed 1000 iterations of the contraction process on each of these configurations. All calculations were performed in double precision.

The rest of this article will be based on results from these configurations; however, we have also done smaller simulations, starting with larger disk areas up to $a = 0.01$. The results of these simulations are in agreement with the results reported here. All errors quoted are statistical errors only, based on linear regression or on standard deviations obtained from fluctuations among the different realizations.

IV. DYNAMICS OF THE ITERATION PROCESS

The increase in the coverage θ as a function of iteration number n is shown in Fig. 3 for the case $a = 0.0002$. The simulations with larger area gave a similar behavior

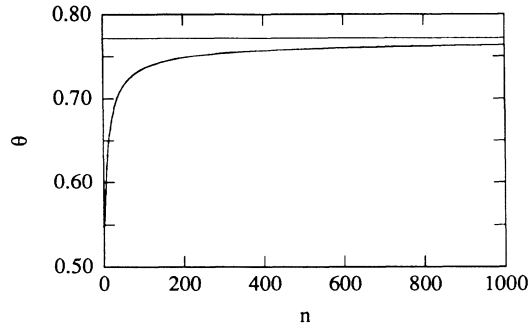


FIG. 3. The coverage θ as a function of iteration number n in the compaction procedure. The horizontal line is the extrapolated limiting value $\theta_\infty = 0.772$.

but on shorter time scales. The iteration number is of course a “nonuniversal” time and should be scaled somehow with the number of particles in the target area to give a size independent time. At the start of the process the average disk movement was 10% of the disk diameter d . After 1000 iterations the average movement was 0.006% of d . The disk diameter had increased with an approximate factor of 1.2 during the iterations. The coverage after 1000 iterations was $\theta = 0.7643 \pm 0.0002$. An example of the initial RSA configuration and the same configuration after 1000 iterations is shown in Fig. 4.

In Fig. 5 we show the change in the standard deviation

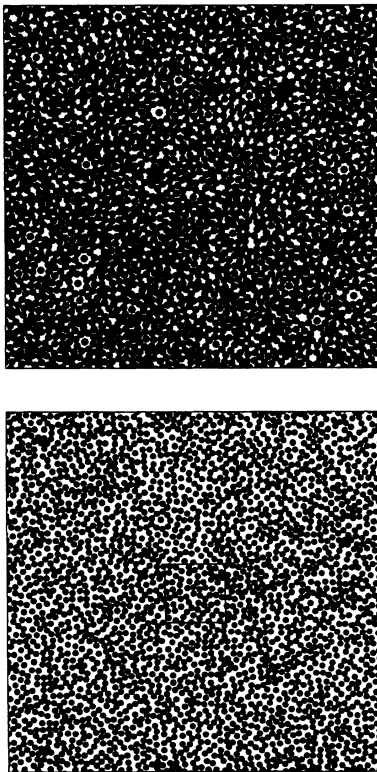


FIG. 4. The top figure shows the starting RSA configuration and the bottom figure shows the resulting configuration after 1000 iterations. The center square in the top figure is enlarged in Fig. 2.

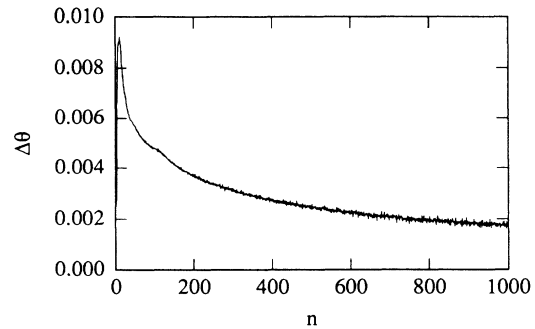


FIG. 5. The standard deviation of the coverage as a function of iteration number.

of the coverage $\Delta\theta = \langle (\theta - \bar{\theta})^2 \rangle^{1/2}$ during the process. We see first a sharp peak, before the standard deviation decreases. Towards the end of the process the decrease in $\Delta\theta$ is approximately proportional to $1/n$. This behavior is easily obtained. We start out with 66 configurations generated by the RSA process described in Ref. 20. These configurations all have the same disk size, but the number of disks on the target area (i.e., the coverage) fluctuates. As the iteration process proceeds the size of the disks is different in different replicas, because in samples with many particles the particle diameter will not increase as fast as in samples with fewer particles. This causes the rms fluctuations to grow. But soon the particle size is adjusted to the particle number, and the fluctuations in the coverage among the different replicas start decreasing. When we stopped the compactification, the rms value had decreased to 67% of the initial value.

The convergence to the limiting state was slow. By fitting the curve in Fig. 3 to various asymptotic functions, we could extrapolate the coverage to infinite iterations. The only functional form that gave a reasonable fit, was a power-law behavior resulting in a coverage $\theta_\infty = 0.772 \pm 0.002$ after an infinite number of iterations. The quality of this fit is shown in Fig. 6 where we have plotted $\log_{10}(\theta_\infty - \theta)$ versus $\log_{10}(1/n)$. We should also mention that during the iteration disk process, holes sufficiently large for an additional disk were created. These were not filled, however. During the later stages of

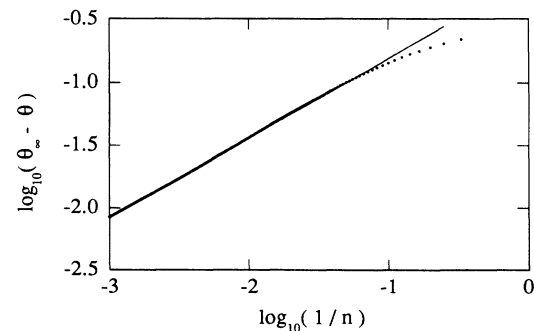


FIG. 6. The coverage $\log_{10}(\theta_\infty - \theta)$ vs $\log_{10}(1/n)$. The straight line is a least-squares fit.

our process, these holes are so rare that filling them at that point would not change the values reported above.

We conclude that the process we have described in Sec. III saturates asymptotically towards a coverage $\theta_\infty = 0.772 \pm 0.002$. In the next section we will argue that this limiting configuration is a random stable configuration with a coverage close to the RLP limit.

V. CORRELATIONS AND STABILITY

The increase in the coverage from $\theta = 0.7634$ after 1000 iterations to the extrapolated value $\theta_\infty = 0.772$ represents an increase in the disk diameter from $d = 1.8847 \times 10^{-2}$ to $d = 1.8953 \times 10^{-2}$ or an increase in the diameter by a factor of 1.006. We claim that there will be no significant changes in the particle positions during the rest of the process. To support this view, we show in Fig. 7 an enlargement of the central region of the configurations in Fig. 4. In the figure we have marked with an arrow the disk movements during the first 300 iterations (top figure) and the last 700 iterations (bottom figure). We see that during the last 700 iterations there has been virtually no movement for most of the disks. What happens is as follows: In each step of the iteration process the radii of the disks are increased uniformly until the first pair of disks reach contact. This pair may be the only pair in contact. The other nearest-neighbor distances are distributed in a narrow peaked distribution. In

the asymptotic limit of the process, the disk pair of closest contact will be slowly separated so that the disk radius may be increased, while all the other disks just “vibrate” around an average position. The average distance a disk is moved in a single iteration step has large fluctuations, but this distance has roughly a $1/n$ dependence towards the end of the process. Most of these movements are, however, vibrational, so the actual displacement of a disk after several iterations falls off more rapidly. The average distance x , a disk has been moved during the first 200 iterations is $x/d = 0.004$, and for the next 200 iterations it is $x/d = 0.0004$. The maximal movement of a disk during the same intervals, is one order of magnitude larger. This process of slowly separating the closest disk pair causes the distribution of nearest-neighbor distances to become sharper. After 200 iterations the peak of this distribution is at $x/d = 1.01$ and after 400 iterations the peak has moved to $x/d = 1.005$. After 1000 iterations it is even closer to 1.

We therefore claim that we can obtain information of the geometrical structure of the limiting configuration by viewing our configurations after 1000 iterations on a clearer scale, that is to say, let the precision in which we can determine the disk diameter d to be accurate to about 0.6%. In practice what we claim is that two disks are in contact when the distance x between them is $x \leq 1.006d$. We now show that under these assumptions our configuration is maximally random and stable.

A. The correlation function

Let $G(r)$ be the two-particle correlation function defined as the probability of finding a disk a distance r from a given disk at the origin (see Ref. 20). In Fig. 8 $G(r)$ is shown for the “limiting” configuration, normalized so that $G(r) \rightarrow 1$ when $r \rightarrow \infty$. The true value of $G(r)$ for $r = d$ is 30, and not 15 as shown in Fig. 8. We reduced the value at contact to a factor of 2 in order to see the structure in the correlation function. The dashed vertical lines in Fig. 8 represent the two-point correlation functions of a triangular lattice. The limiting configuration has no long-range order, since $G(r) \approx 1$ for $d > 3$. For $d < 3$ we see some structure reminiscent of the triangular lattice. However, the peaks in the correlation function are far

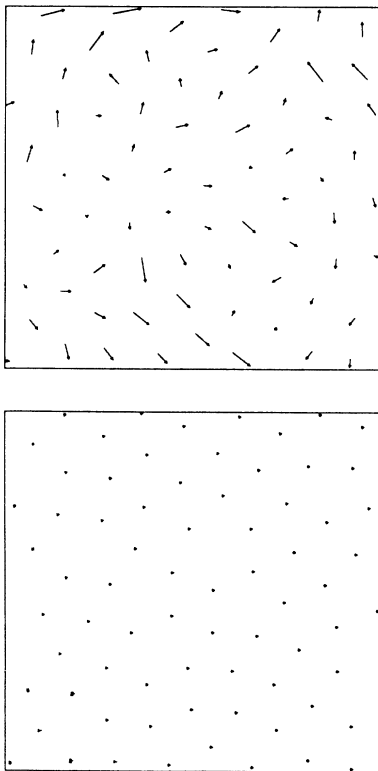


FIG. 7. The figure shows the movements of the disks in Fig. 2 during the iteration process. The top figure shows the movement during the first 300 iterations, and the lower figure shows the movement during the last 700 iterations.

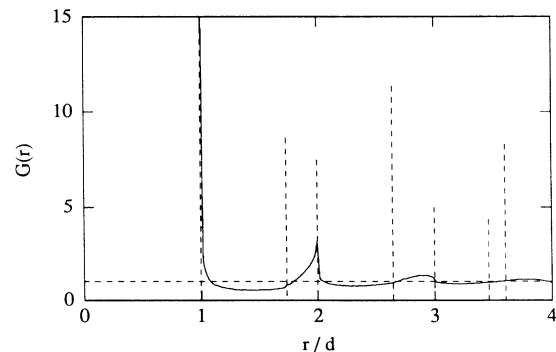


FIG. 8. The two-point correlation function. The dashed vertical lines are the two-point correlation functions for the triangular lattice.

less pronounced and localized than the peaks in the correlation function obtained by Mason³⁷ at the same coverage. Also the correlation function presented by Schreiner²⁹ have pronounced peaks at the position of the δ function peaks for a CP configuration (see Fig. 8), so it is doubtful that their configurations are maximally random.

B. The geometrical neighbors

To test the short-range correlations further, we have measured the distance to the geometrical neighbors^{3,20} defined by the VD tessellation. The distance to the first-second- and third-neighbor disk have δ -function-like distributions. This is because at least three disks support a given disk, except disks which are free to move in rigid surroundings as mentioned earlier. These local configurations broaden the distribution slightly, as seen in Fig. 9. The distance to the fourth and fifth nearest geometrical neighbor yield broader distributions, but still with a value greater than zero at $x/d = 1$, as shown in Fig. 9. In order to have a reasonable scale on the ordinate axis in Fig. 9, we have reduced the value at the point $x = d$. The correct value for the first point in the first-, second-, and third-neighbor disk distributions are 92.7 and 32.7 for the fourth distribution. The sixth-neighbor distance distribution has a value approximately zero for $x/d = 1$ as seen in Fig. 9. This implies that no local hexagonal configurations exist. We have therefore no short-range order either. The configuration we have generated is therefore maximally random.

C. Stability

The *coordination number* z is defined as the average number of geometrical neighbors in contact with a given disk. Bideau *et al.*²⁸ showed that for a configuration with maximal disorder, $z = 4$ is an upper limit of the coordination number. Their argument is as follows: Start with the network defined from *the real contacts* between disks. This implies a network consisting of polygons which have edges of equal length d . From the Euler-Poincaré theorem²⁰ one can write

$$\left[\sum_{n \geq 3} P_n \right] - E + N = 1, \quad (1)$$

where P_n is the number of n -sided polygons, E is the total number of edges of these polygons, and N is the number of disks, or equivalently, the number of vertices in the tessellation. Using the fact that each edge is defined by two polygons, and that an edge ends at two vertices, one may write $\sum_{n \geq 3} n P_n = 2E = Nz$. Substituting the last part of this relation in Eq. (1), gives

$$\sum_{n \geq 3} P_n = N(z - 2)/2, \quad (2)$$

where a term of order 1 has been neglected. Since all edges in the tessellation have the same length d , a polygon P_n with n sides, is completely determined by specifying $(n - 3)$ angles. The full tessellation is then specified by determination of $\sum_{n \geq 3} (n - 3)P_n$ angles. In addition there are N constraints at each vertex stating that the sum of angles is 2π . For the packing to be maximally random (or maximally disordered), the number of angles must be larger than the number of constraints,

$$\sum_{n \geq 3} (n - 3)P_n \geq N. \quad (3)$$

If this was not the case, there would be correlations between the angles. Using the above relations, Eq. (3) is equivalent to $z \leq 4$.

Uhler and Schilling⁴⁴ tried to give an estimate of the coordination number for a loose-packed configuration by calculating the probability of a disk having n neighbors in contact in a stable configuration. The central disk is stable if it cannot move without moving any of its neighbors. The value they obtained was $z \approx 3.3 - 3.4$. Even though their calculation was rather general in connection with the process producing the random packing, it still assumed a growth process of the packed configuration disk by disk. Therefore this bound does not prevent the coordination number from being lower in a cooperative packing procedure like the one we have implemented here.

In Fig. 10 we show how the coordination number changes as the precision used to determine the disk diameter d changes. The lowest curve is the RSA configuration, and the other curves show the development for iteration number $n = 200, 400, 600, 800,$ and 1000 . From these curves we extrapolate that the configuration in the limit $n \rightarrow \infty$ has a coordination number $z = 3.00 - 3.05$.

We find that each disk is supported by three disks not all on the same side of a big circle, except for the disks which are free to move in a surrounding enclosed by a rigidly locked structure. Stillinger *et al.*⁸ argued that these locked structures are local configurations which would rarely appear. Our procedure, however, generates such configurations rather frequently, as can be seen in the lower part of Fig. 4. This is a somewhat surprising feature. The existence of many local configurations like these is probably the reason why our configuration is at the lower limit of stability, and that the coverage is low. Even if the free disks are moved, only few additional disks may be added to the configuration, so that the value

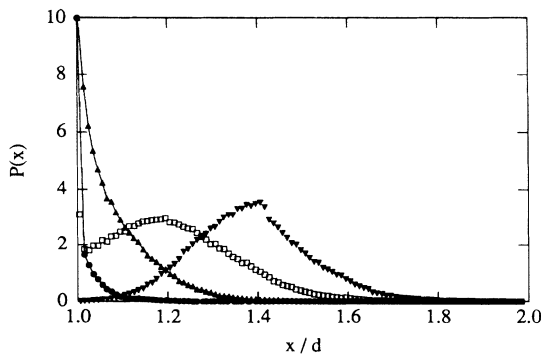


FIG. 9. The probability density of finding a geometrical neighbor at a distance x/d . ●: First-, second-, and third-neighbor distributions collapse into the same curve; ▲: fourth-neighbor; ◻: fifth-order neighbor; and ▼: sixth-neighbor.

of the extrapolated coverage will be approximately the same. Oger *et al.*⁴⁵ have studied the same effect of local arching in three-dimensional packings created in a collective rearrangement process.

The topological relations used to derive the constraint $z \leq 4$ for a maximal random packing, was also used by Bideau *et al.*²⁰ to obtain an expression for the coverage. If A_n is the average area of a polygon with n sides, the coverage may be written as

$$\theta = \frac{\pi \langle d^2 \rangle}{4 \sum_{n \geq 3} P_n A_n}. \quad (4)$$

Here $\langle d^2 \rangle$ is the average squared particle diameter, if the packing has a size distribution of disks. Eliminating P_3 and P_4 between Eqs. (1) and (2) gives

$$\theta = \pi \langle d^2 \rangle / 4 \left\{ A_4 + \frac{4-z}{2} (A_4 - 2A_3) + \frac{1}{N} \sum_{n \geq 5} P_n [A_n - (n-3)A_4 + (n-4)A_3] \right\}. \quad (5)$$

For a packing of equal-sized disks, the polygons with three edges are all equilateral triangles with area $A_3 = d^2 \sqrt{3}/4$. The polygons with four sides are rhombii with angles between $\pi/3$ and $2\pi/3$. The average area of these, assuming an uniform distribution of angles, is $A_4 = d^2 3/\pi$. Inserting this in Eq. (5) leads to

$$\theta = \frac{\pi^2}{12} \left[1 + \frac{4-z}{2} \left[1 - \frac{\pi\sqrt{3}}{6} \right] + \frac{1}{N A_4} \sum_{n \geq 5} P_n [A_n - (n-3)A_4 + (n-4)A_3] \right]^{-1}. \quad (6)$$

Bideau *et al.*²² studied numerically a packing generated from a seed in a central field according to the algorithm of Bennet.⁵ In this case over 70.1% of the polygons had four edges, and 20.7% of the polygons had three edges. From this simulation they concluded that the sum in Eq. (6) was less than a 0.5% correction term compared with $N \times A_4$. Since $z=4$ is believed to be an upper bound for the coordination number of a maximal random configuration, it follows from Eq. (6) that an RCP configuration should have a coverage close to $\theta = \pi^2/12 = 0.822$. This value is then an upper limit for a maximal random packing, and the coverage corresponds to only taking into account the contributions from the rhombii. Gamba⁴¹ and Bordia⁴³ took only this contribution into account in their derivation of the packing fraction. It is interesting to observe that with a coordination number of $z=3$, Eq. (6) leads to a coverage $\theta = 0.786$ as an upper limit. Taking into account a 0.5% correction from the sum, the coverage becomes $\theta = 0.782$. This is close to the average $\theta_\infty = 0.772$ that we found for the limiting configurations of our compaction algorithm.

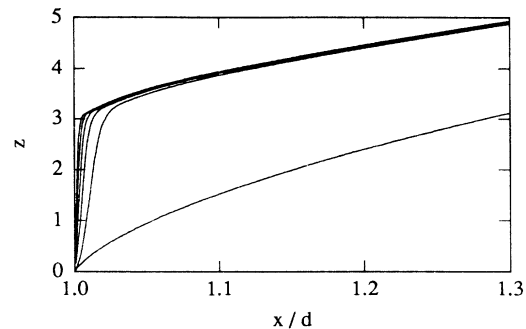


FIG. 10. The figure shows how the coordination number changes as the precision used to specify the side diameter changes. The lower curve is for the initial RSA configuration. The other curves show the behavior after 200, 400, 600, 800, and 1000 iterations.

We conclude that the configurations we have generated are stable and dense in the limit of infinite iterations. Since the coordination number z of our configuration is at the lower limit of stability, with a coverage $\theta_\infty = 0.772 \pm 0.002$, we suggest that the value we have obtained must be very close to the RLP coverage.

VI. HOLE-SIZE DISTRIBUTION

In Ref. 20 we introduced the concept of circular holes. There we showed the existence is a one-to-one correspondence between the circular holes and the vertices of the VD network. In Fig. 11 we have plotted the probability distribution for these holes. We see that the distribution has two regions where it decreases in a characteristic fashion. The lower cutoff value corresponds to the smallest possible hole, defined by three disks with three points of contact. The crossover value is very close to the largest hole defined by three disks with two points of contact.

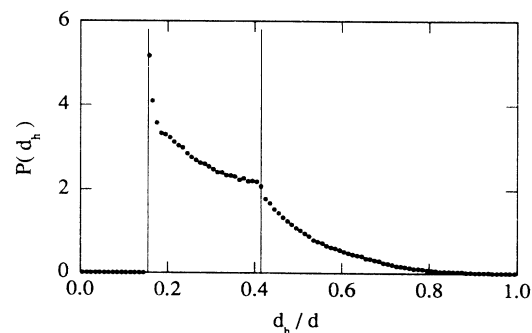


FIG. 11. The hole-size distribution function. The first vertical line is the diameter of the smallest hole possible, and the next is the diameter of the largest hole defined by three disks with two points of contact.

This is the largest stable hole possible where the disks have some points of contact. Many holes bigger than this value would imply that the configuration was unstable. As can be seen, the number of holes with a diameter larger than d , is virtually zero. The actual number was 1.7 holes per sample.

VII. STATISTICS OF THE VD DIVISION OF SPACE

Of the three different networks that may be assigned to a disk packing, we have chosen to concentrate on the VD network, the reason being that the limiting configuration is not reached. From the discussion of the disk movements in Sec. V, it follows that the change in the statistics of the VD polygons between the configurations after 1000 iterations and the limiting configuration is minimal. We have compared the statistics at several stages of the iteration process, and above $n=400$ there are hardly any changes at all. But if we had used the network based on real contacts, the change would have been very large. The method of relaxing the criterion of contact, as explained in Sec. V is problematic. The value found in Sec. V is based on an average over many samples. The correct statistics is probably not found by using an average value for the individual samples due to the problem of dangling and unconnected bonds. These considerations made us feel uncertain about the statistics based on this network. In Fig. 12 we have plotted the distribution functions of area A , circumference O , edges L , and angles ϕ of the polygons in the VD network. The normalization is such that the integrals of the distributions are 1. Both for the area and the circumference we made fits to a Γ distribution

$$P(x) = \frac{1}{\Gamma(\nu)(\bar{x}/\nu)^\nu} x^{\nu-1} \exp[-\nu(x/\bar{x})], \quad (7)$$

where \bar{x} is the mean value of the distribution. The value of x in the distribution functions are $x = (A - A_{CP})/a$ and $x = (O - O_{CP})/o$. $A_{CP} = \sqrt{3}d/2$ and $O_{CP} = 2\sqrt{3}d$ are the area and the circumference, respectively, of a VD polygon in a closed-packed configuration, and $a = \pi d^2/4$ and $o = \pi d$ is the area and the circumference of a disk, respectively. The parameters in the fit are $\nu=5.5$ and $\bar{x}=0.21$ for the area distribution, and $\nu=6.6$ and $\bar{x}=0.14$ for the distribution of circumference. The Γ distribution was earlier found to fit the distribution of cell areas in a VD tessellation defined from completely random points.⁴⁶ The value of ν found for these area distributions was close to 3.6, and is lower than the value we obtained for our distributions.

It has not been claimed that the Γ distribution is an exact result for the case of random points on a plane, even though the quality of the fits are very good. Neither do we believe that this is the case for our configurations. However, the important point to notice is that such a fit gives additional quantitative information beyond the qualitative shape of the distribution. As pointed out earlier, statistical distribution of network quantities are one of the main tools in characterizing a random geometry. Such additional quantitative information is therefore valuable in order to compare different random

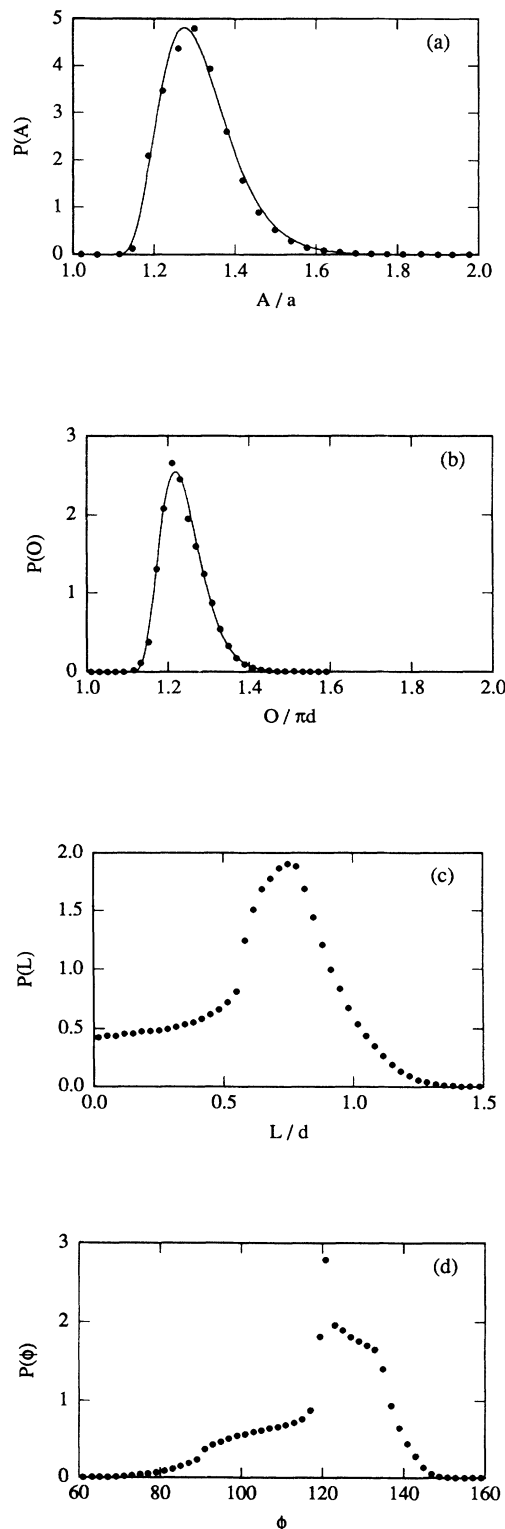


FIG. 12. Distribution functions for the VD polygons for the compacted configuration. (a) Distribution of polygon area A normalized with the disk area a . (b) Distribution of polygon circumference O normalized with the disk circumference $O = \pi d$. (c) Distribution of polygon sides L normalized with disk diameter d . (d) Distribution of polygon angles ϕ . The curves in (a) and (b) are fit to Γ distributions.

TABLE I. The frequencies of VD polygons occurring in the compacted configuration.

No. of edges	Occurrence (%)
3	0.0
4	0.252
5	21.593
6	56.999
7	20.224
8	0.920
9	0.011
10	0.0
Total	99.999

geometries. It is also possible that there exist geometries where a fit to a Γ distribution is ruled out.

In Table I we list the frequencies of the different VD polygons occurring in our configurations. We see that only 57% of the polygons have six sides, this being slightly higher than the value 50% in the RSA configuration. The average number of sides is however 6.00, consistent with the constraints derived from the Euler-Poincaré theorem.

VIII. CONCLUSION

We have studied a compaction process of a surface filled with nonoverlapping disks, and characterized the resulting geometry. We started out with a surface jammed with disk generated by the random sequential adsorption algorithm. The coverage of the RSA configurations at the jamming limit was $\theta=0.5472\pm 0.0002$, and is the most precise value reported so far. This configuration was compacted using an algorithm designed to keep the packing uniformly random during the hole process. At each stage of the compaction process, we constructed the Voronoi-Dirichlet tessella-

tion, and moved every disk to the center of the largest circle which could be inscribed in a VD polygon. The disk diameters were expanded until the first pair of disks was in contact, then the iteration was repeated. A random dense-packed configuration with coordination number $z=3.00-3.05$ was the limiting configuration in the limit of infinitely many iterations of the compaction procedure. This value is at the lower limit of stability. The coverage obtained was $\theta=0.772\pm 0.002$. We have argued that this limiting configuration is stable, implying that the obtained coverage should be close to the coverage of an RLP configuration. The coverage for the compacted packing is close to a predicted coverage of $\theta=0.78$ based on a formula developed by Bideau *et al.*²⁸ Our method of compaction is a collective rearrangement process. As a result, many local configurations containing one or a few disks free to move in a rigidly locked environment were created. Such local configurations cannot be created in a process where individual disks are packed one by one. Several statistical distributions calculated from the limiting geometry of the compaction algorithm was studied. We found that both the area and circumference distributions of the Voronoi-Dirichlet polygons could be fitted to Γ distribution functions. The disk packings generated by our algorithm are well characterized and suitable as "substrates" for the study of physical phenomena such as the flow of fluids in porous media. Together with the random sequential adsorption and the random close-packed configurations they form a series of well-characterized random configurations at different coverage and porosities.

ACKNOWLEDGMENTS

We thank P. Meakin and U. Oxaal for very helpful and stimulating discussions. This work has been supported by VISTA, a research cooperation between the Norwegian Academy of Science and Letters and Den Norske Stats Oljeselskap a.s. (STATOIL).

- ¹J. Kepler, *De Congruentia Figurarum Haromanicarum*, Vol. II of *Harmonices Mundi* (1619), (Beck, Munich, 1940).
- ²J. D. Bernal, Proc. R. Soc. London Ser. A **280**, 299 (1964); G. S. Cargill III, Solid State Phys. **30**, 227 (1975); J. L. Finney, Nature **266**, 309 (1977); M. Dixmier, J. Phys. (Paris) **39**, 873 (1978); B. Bagchi, C. Cerjan, and S. A. Rice, Phys. Rev. B **28**, 6411 (1983).
- ³R. Zallen, *The Physics of Amorphous Solids* (Wiley, New York, 1983).
- ⁴J. L. Finney, Proc. Roy. Soc. London Ser. A **319**, 479 (1970); J. L. Finney, *ibid.* **319**, 495 (1970).
- ⁵C. H. Bennett, J. Appl. Phys. **43**, 2727 (1972).
- ⁶M. Shahinpoor, Powder Technol. **25**, 163 (1980).
- ⁷D. P. Haughey and G. S. G. Beveridge, Can. J. Chem. Eng. **47**, 130 (1969); R. Omnes, J. Phys. (Paris) **46**, 139 (1985); L. Oger, E. Guyon, and D. Wilkinson, Europhys. Lett. **4**, 301 (1987); L. Oger, E. Guyon, and T. Plona, Acta Stereol. **6/III**, 425 (1987).
- ⁸F. H. Stillinger, Jr., E. A. Dimarzio, and R. L. Kornegay, J.

Chem. Phys. **40**, 1564 (1964).

⁹J. A. Dodds, Nature **256**, 187 (1975); **266**, 614 (1977).

¹⁰J. G. Berryman, Phys. Rev. A **27**, 1053 (1983).

¹¹D. Bideau and J. P. Troadec, J. Phys. C **17**, L731 (1984).

¹²D. E. G. Williams, J. Phys. C **18**, L181 (1985).

¹³G. T. Barnes, T. I. Quickenden, and J. Saylor, J. Coll. Interface Sci. **33**, 236 (1970).

¹⁴H. H. Kausch, D. G. Fesko and N. W. Tschoegl, J. Coll. Interface Sci. **37**, 603 (1971).

¹⁵T. I. Quickenden and G. K. Tan, J. Coll. Interface Sci. **48**, 382 (1974).

¹⁶J. Feder and I. Giaever, J. Coll. Interface Sci. **78**, 144 (1980).

¹⁷M. Shahinpoor, J. Coll. Interface Sci. **85**, 227 (1982).

¹⁸K. J. Mäløy, J. Feder, and T. Jøssang, Phys. Rev. Lett. **55**, 2688 (1985).

¹⁹L. Finegold and J. T. Donnell, Nature **278**, 443 (1979).

²⁰E. L. Hinrichsen, J. Feder, and T. Jøssang, J. Stat. Phys. **5/6**, 813 (1986).

²¹M. Hasegawa and M. Tanemura, Ann. Inst. Stat. Math. **28B**,

- 509 (1976).
- ²²D. Bideau, A. Gervois, L. Oger, and J. P. Troadec, *J. Phys. (Paris)* **47**, 1697 (1986).
- ²³G. D. Scott and D. M. Kilgour, *Br. J. Appl. Phys.* **2**, 863 (1969).
- ²⁴J. L. Finney, *Mater. Sci. Eng.* **23**, 199 (1976).
- ²⁵K. Gotoh and J. L. Finney, *Nature* **252**, 202 (1974).
- ²⁶G. S. Cargill III, in *Physics and Chemistry of Porus Media*, Proceedings of a Symposium on the Physics and Chemistry of a Porus Media, AIP Conf. Proc. No. 107, edited by D. L. Johnson and P. N. Sen (AIP, New York, 1984).
- ²⁷W. M. Visscher and M. Bolsterli, *Nature* **239**, 504 (1972).
- ²⁸D. Bideau, J.-P. Troadec, and L. Oger, *C. R. Acad. Sci. Paris* **297**, 319 (1983); **297**, 219 (1983).
- ²⁹W. Schreiner and K. W. Kratky, *J. Chem. Soc. Faraday Trans. 2* **78**, 379 (1982).
- ³⁰D. R. Nelson, *Phys. Rev. B* **28**, 5515 (1983).
- ³¹M. Rubinstein and D. R. Nelson, *Phys. Rev. B* **28**, 6377 (1983).
- ³²M. Rubinstein and D. R. Nelson, *Phys. Rev. B* **26**, 6254 (1982).
- ³³D. R. Nelson, M. Rubinstein and F. Spaepen, *Philos. Mag. A* **46**, 105 (1982).
- ³⁴D. M. Livesley and J. N. Loveday, *Philos. Mag. A* **53**, 595 (1986).
- ³⁵M. Ammi, D. Bideau, and J. P. Troadec, *J. Phys. D* **20**, 424 (1987).
- ³⁶V. C. Aguilera-Navarro, M. Fortes, M. de Llano, and A. Platinio, *J. Chem. Phys.* **76**, 749 (1982).
- ³⁷G. Mason, *J. Coll. Interface Sci.* **56**, 83 (1976).
- ³⁸G. A. Slack, *Z. Krystallogr.* **85**, 1 (1983).
- ³⁹H. Kuno, *J. Jpn. Soc. Powder Metall.* **19**, 85 (1972).
- ⁴⁰J. W. Ross, W. A. Miller, and G. L. Weatherly, *Acta Metall.* **30**, 203 (1982).
- ⁴¹A. Gamba, *Nature* **256**, 521 (1975).
- ⁴²D. N. Sutherland, *J. Coll. Interface Sci.* **60**, 96 (1977).
- ⁴³R. K. Bordia, *Scr. Metall.* **18**, 725 (1984).
- ⁴⁴W. Uhler and R. Schilling, *J. Phys. C* **18**, L979 (1987).
- ⁴⁵L. Oger, J. P. Troadec, D. Bideau, J. A. Dodds and M. J. Powell, *Powder Technol.* **46**, 121 (1986).
- ⁴⁶D. Weaire, J. P. Kermode, and J. Wejchert, *Philos. Mag. B* **53**, L101 (1986).